

The Influence of Ultra-High-Energy Cosmic Rays on Star Formation in the Early Universe

E. O. Vasiliev and Yu. A. Shchekinov*

Rostov State University, Rostov-on-Don, Russia

Received July 3, 2004; in final form, April 14, 2006

Astronomy Reports, 2006, Vol. 50, No. 10, pp. 778-784. Original Russian Text published in Astronomicheskii Zhurnal, 2006, Vol. 83, No. 10, pp. 872-879.

Abstract

The presence of ultra-high-energy cosmic rays (UHECR) results in an increase in the degree of ionization in the post-recombination Universe, which stimulates the efficiency of the production of H₂ molecules and the formation of the first stellar objects. As a result, the onset of the formation of the first stars is shifted to higher redshifts, and the masses of the first stellar systems decrease. As a consequence, a sufficient increase in the ionizing radiation providing the reionization of the Universe can take place. We discuss possible observational manifestations of these effects and their dependence on the parameters of UHECR.

1 INTRODUCTION

One of the scenarios [1, 2, 3] for the formation of ultra-high-energy cosmic rays (UHECR, with energies above the Greisen-Zatsepin-Kuzmin cut-off, $E > 10^{20}$ eV, [4, 5]) suggests they are formed due to the decay of ultra-heavy X particles with masses $\geq 10^{12}$ GeV. In the interaction of UHECR with low-energy cosmic-microwave background (CMB) photons and the subsequent electromagnetic cascades, resonance and ionizing photons are emitted, which can increase fractional ionization of the matter in the post-recombination Universe at redshifts $\sim 10 - 50$ by factors of 5–10 compared to the standard recombination regime. This circumstance could qualitatively change the entire subsequent evolution of the Universe, since the degree of ionization substantially influences the rate of radiative cooling by gas, and hence, the formation of the first stellar objects. Indeed, cooling of the primordial gas at low temperatures $T < 10^3$ K is provided by thermal radiation in rotational lines of H₂. In turn, H₂ molecules can form in the primordial gas only via ion-molecule reactions involving H⁺ and H₂⁺, in which electrons and protons play the role of catalysts [8].

Thus, the presence of UHECR in the early Universe can appreciably influence the subsequent stellar phase of its evolution. For this reason, observational manifestations connected with characteristic features this phase can be used to constrain the parameters of UHECR. In the present paper, we show that due to the influence of UHECR stellar evolution in the Universe begins at earlier epochs, and discuss possible observational consequences of this prediction. Section 2 describes the ionization and molecular kinetics of baryons in dark halos and their thermodynamics in the presence of cosmic rays. In Section 3, we present and discuss our results. A summary is given in Section 4. In calculations we assumed a Λ -CDM model for the Universe: $(\Omega_0, \Omega_\Lambda, \Omega_m, \Omega_b, h) = (1.0, 0.71, 0.29, 0.047, 0.72)$ and deuterium abundance $n[D]/n = 2.6 \times 10^{-5}$ [9].

*yus@phys.rsu.ru

2 COSMIC RAYS AND THE THERMO-CHEMICAL EVOLUTION OF BARYONS IN DARK HALOS

Interaction of UHECR with CMB photons produces high-energy particles – photons, electrons, positrons, and neutrinos, which transform through electromagnetic cascades into ionizing Lyc and resonant Ly α photons at the rate (per unit volume) [6, 10]

$$\frac{dn_{i,r}}{dt} = \epsilon_{i,r}(z)H(z)n. \quad (1)$$

Here, $H(z)$ is the Hubble constant, n is the baryon density,

$$\epsilon_{i,r} \simeq \frac{2.5 \times 10^{-4}}{1+z} M_{16}^{2-\alpha} \Theta_{tot}, \quad (2)$$

is the efficiency of production of ionizing and resonant photons [6], where α is the spectral index of the photon spectrum produced in the decay of a superheavy particle, $M_{16} = M_X/10^{16}$ GeV, M_X is the mass of the superheavy particle, Θ_{tot} is a function determined by the rate of decay of superheavy particles at the present epoch and its redshift dependence [6, 11]. For the cosmic rays to produce measurable distortions of the CMB radiation, the function Θ_{tot} must be of the order of $\simeq 10^4 M_{16}^{-0.5}$ [6]. Following [7], we assume that the efficiencies of producing resonant and ionizing photons are similar: $\epsilon_r(z) = \epsilon_i(z) = \epsilon/(1+z)$.

In the standard model of the Universe, in the post-recombination period ($z \simeq 1100$) before the formation of the first stars ($z \simeq 30 - 20$), there are no sources of ionizing photons. In these conditions, fractional ionization $x = n[\text{H}^+]/n$ is determined by photo-recombinations, and ionization by additional Lyc and Ly α photons produced by the cosmic rays

$$\dot{x} = -k_1 n x^2 + \frac{\epsilon}{1+z} H(z)(1-x). \quad (3)$$

Under such conditions, the rate of formation of molecular hydrogen, $f = n[\text{H}_2]/n$, is given by the expression

$$\dot{f} = k_m n(1-x-2f)x, \quad (4)$$

where

$$k_m = \frac{k_2 k_3}{k_3 + k_4/(1-x)n} + \frac{k_5 k_6}{k_6 + k_7/(1-x)n}, \quad (5)$$

is the reduced rate of convergence of H into H₂ [12] and k_i are the rates of intermediate reactions (see the table). At low temperatures ($T < 200$ K), HD molecules can substantially influence the thermal state of the gas [18, 19]. The kinetics of these molecules is described by the equation

$$\dot{g} = k_{D1} f x n d_c - n x (k_{D1} f + k_{D2}) g, \quad (6)$$

where $g = n[\text{HD}]/n$ is the number density of HD molecules, $d_c = n[\text{D}]/n$ is the deuterium abundance, and k_{D1} and k_{D2} are the rates of formation and destruction of HD [17].

The growth of initial perturbations in the dark matter leads to the formation of gravitationally bound objects – so called dark halos, in whose potential wells baryons come into virial equilibrium, and later on cool radiatively and give birth to stars.

The role of UHECR at the initial star-formation stage is determined by their influence on the thermal state of the baryons. In order to understand this role, we consider the evolution of baryons in a virialized halo using the simple system of equations (see, for instance, [20])

$$\dot{R} = u, \quad (7)$$

$$\dot{u} = \frac{4kT}{\mu m_p R} - \frac{4}{3}\pi G(\rho_d + \rho)R, \quad (8)$$

$$\dot{T} = -\frac{2kT}{3\mu R}u - \Sigma\Lambda_i, \quad (9)$$

where $n = \rho/\mu m_p$, ρ_d is the density of dark matter, R is the radius of the region occupied by baryons, u is the velocity of the boundary of the baryon cloud, Λ_i are the cooling/heating rates due to Compton interactions with the CMB photons and radiation in lines of atomic and molecular hydrogen and HD molecules (expressions for the cooling/heating rates are given in [21]). The initial values of the radius and temperature were assumed to be equal to the virial values for a given halo mass. The number densities of electrons and of H₂ and HD molecules were calculated for the virialization time, assuming a simple prescription for the evolution of the density perturbation [12].

3 RESULTS

Figure 1 shows the z dependences of the temperature, density, and Jeans mass of the gas for three halos with the masses of $10^6 M_\odot$, $10^7 M_\odot$, and $10^8 M_\odot$ that have reached a virial state at redshift $z = 20$, and for three values of the production efficiency of ionizing photons from cosmic rays ($\epsilon = 0, 0.1, 1$). As an example, let us consider in more detail the evolution of a $10^7 M_\odot$ halo. In the model with cosmic rays, the number density of electrons at the virialization time increases by approximately a factor of five. As a result, the number density of H₂ molecules substantially increases: during the contraction of the baryons, it is 4×10^{-4} at $z = 16.5$ for the model with $\epsilon = 0$, while for $\epsilon = 0.1$ it is already 3×10^{-3} . As a result, in the models with non-zero ϵ , the gas temperature falls faster, and becomes lower for lower densities. A fairly high abundance of molecular hydrogen already at the beginning of the contraction, together with low temperature, favors binding almost all the deuterium in HD molecules, due to the effects of chemical fractionation [18]. When $T < 200$ K, the main input to the cooling process is provided by HD molecules, and the cooling is then so strong that the temperature drops rapidly, and attains the CMB temperature, ~ 50 K. HD molecules provide efficient heat exchange between the CMB radiation and baryons via absorption of CMB photons and subsequent transfer of the excitation energy to the gas in collisional processes [18]. As a result, the baryon contraction becomes isothermal. The gas density grows rather rapidly, and starting from the value $\geq 3 \times 10^7 \text{ cm}^{-3}$, the optical depth in the HD lines exceeds unity. The Jeans mass varies as $M_J \sim 100(1+z)^{3/2}n^{-1/2}M_\odot$, and reaches $\sim 1 - 2 M_\odot$. At higher densities, three-particle collisions become the major mechanism for forming H₂, and at $n \sim 10^{8-9} \text{ cm}^{-3}$ the abundance of H₂ becomes ~ 1 . Thus, the central regions of the cloud become opaque in H₂ lines [22, 23].

Halos with lower masses evolve much slower, but as the efficiency of producing ionizing photons increases, the abundances of electrons and H₂ and HD molecules also increase, the temperature decreases substantially, and the halo begins to contract isothermally but at higher temperatures. For example, in the model without cosmic rays, the temperature of a $10^6 M_\odot$ halo in this regime is $T \sim 300$ K, which can be explained by the less efficient formation of H₂ and HD molecules. Thus, the transition of a halo to isothermal contraction is determined by its mass.

Let us consider the dependence of the redshift z_t at which the transition to isothermal contraction occurs, on the halo-virialization epoch z_v and the efficiency ϵ , using as an example a halo with mass $M_{3\sigma}$ and with a perturbation amplitude corresponding to the 3σ level (see, for example, [24]). Figure 2 shows the dependence $z_t(z_v)$ for $\epsilon = 0, 0.1, 1$. The upper x axis shows the masses of perturbations with amplitudes exceeding 3σ that result in the formation of halos with mass of $M_h = M_{3\sigma}$ at z_v ; the formation of halos with $M_h > M_{3\sigma}$ has low probability. It is seen that for larger ϵ the halos evolve more rapidly to the isothermal regime, particularly in the low-mass end. As the halo mass increases, the effect of decrease of the time needed to attain the isothermal state weakens, since cooling and

contraction to high densities are possible in massive halos due to energy losses in lines of atomic hydrogen.

Thus, the presence of UHECR substantially accelerates the halo evolution. With increasing ϵ , the contraction of the gas proceeds much more rapidly: with $\epsilon = 0$, the baryons in a $10^7 M_\odot$ halo virialized at $z = 20$ converge to isothermal contraction at $z \approx 13.5$, while for $\epsilon = 3$ this transition occurs at $z \approx 17$. The influence of cosmic rays on the thermal evolution can play a principal role for lower-mass halos. For instance, when $\epsilon = 0$, halos with $M_h \simeq 3 \times 10^6 M_\odot$ attain an isothermal state only by $z \sim 7$, when the flux of external UV photons produced by the stellar populations of more massive halos becomes sufficiently strong for the temperature of the baryons in such low-mass halos to exceed the virial temperature, and for star formation to be suppressed [24, 25]. However, when $\epsilon = 0.1$, such halos converge to the isothermal regime much earlier – at $z \simeq 12$, when the influence of the ionizing radiation from massive halos is negligibly small. Large values of ϵ result not only in a general acceleration of the evolution of halos of all masses, but also in a shift of the minimum mass M_{\min} for the most rapidly evolving halos; this mass corresponds to the maxima of the curves for different values of ϵ values in Fig. 2. When $\epsilon \simeq 1$, the gas in halos with masses $5 \times 10^6 M_\odot$ attains the isothermal regime and conditions favorable for star formation already by $z \approx 15$ (Fig. 2), i.e. long before the influence of earlier formed low-mass halos can become important, while larger-mass objects form later, so that their radiation cannot affect the evolution of lower-mass halos. Thus, the influence of UHECR is critical for low-mass halos: in the presence of UHECR, the masses of halos in which star formation is possible decrease and a larger baryon fraction of the Universe becomes involved into stellar evolution. Further, their stellar population can substantially change the ionization and thermal state of the gas, since in the hierarchical scenario of galaxy formation low-mass objects contain a larger fraction of the mass. This circumstance may turn out to be of a fundamental importance for interpretation of the Wilkinson Microwave Anisotropy Probe (WMAP) data [9].

According to the WMAP measurements of the background polarization, the optical depth of the Universe to Thomson scattering is $\tau_e = 0.16$ [26]. Such a high value corresponds to the beginning of the reionization of the Universe at a redshift of $z = 17$ [26]. On the other hand, the spectra of distant quasars show that reionization was completed only by $z \sim 6$ [27, 28]. In addition, the flux of ionizing UV radiation expected from quasars and young galaxies is insufficient to reionize the Universe, even if the mass distribution of stars, i.e., the initial mass function in the early Universe, was skewed towards higher masses. Additional sources of ionizing photons, such as the radiation of accreting black holes [29, 30], radiation from microquasars [31], and the decay of unstable neutrinos [32, 33, 34], have been recently considered to explain the early reionization. In these conditions, the increase of the fraction of baryons condensed into stellar phase at the initial star formation stage in the Universe, f_* , is an important factor in providing the necessary rate of reionization. In the presence of UHECR, this fraction certainly grows, due to the increase in the efficiency of radiative cooling of the baryons. Figure 3 shows the dependence of

$$f_* = \frac{\int_{M_{\min}(z, \epsilon)}^{\infty} \psi(M) dM}{\int_{M_{\min}}^{\infty} \psi(M) dM} \quad (10)$$

on ϵ , where $\psi(M)$ is the fraction of baryons present in stars within mass M , calculated using the formalism [35] [see (12) below], M_{\min} is the lower limit of masses of dark halos, and $M_{\min}(z, \epsilon)$ is the minimum mass of the dark halos that are able to cool and form stars. The corresponding z dependence of the number of ionizing photons f_{uvpp} per baryon associated with stellar nucleosynthesis is shown in Fig. 3. It is seen from this dependence that at the supposed epoch of reionization of the Universe ($z \leq 15$), the number of ionizing photons in models with $\epsilon \neq 0$ can increase by half an order of magnitude. Thus, the full reionization of the Universe may be determined by the stimulating effect of UHECR on characteristics of the initial stage of stellar nucleosynthesis.

The presence of UHECR in the early Universe may be revealed from the properties of the characteristic molecular-line emission arising in the stages preceding formation of the first stars. At the

prestellar stage, dense and cold gaseous condensations and molecular clouds form in dark halos, with substantial energy losses in H₂ and HD lines. The total energy released in rotational lines of H₂ and HD may be $\epsilon_{\text{H}_2} \sim 10^{12} \text{ erg g}^{-1}$. The total emission from such molecular clouds in galaxies with masses $10^9 - 10^{11} M_\odot$ can be substantial, and sufficient to be detected by the planned infrared and submillimeter telescopes ALMA¹, ASTRO-F² and SAFIR³. The influence of UHECR will be manifested as an increase in the relative specific energy release in H₂ and HD lines

$$\langle E_{\text{H}_2} \rangle = \frac{\int_{M_{\text{min}}(z, \epsilon)}^{\infty} \epsilon_{\text{H}_2} \psi(M) dM}{\int_{M_{\text{min}}}^{\infty} \psi(M) dM}, \quad (11)$$

as well as an increase in the redshift at which this emission is detected, z_{H_2} . This dependence is shown in Fig. 4. An unambiguous relationship between the observable quantities $\langle E_{\text{H}_2} \rangle$ and z_{H_2} and the parameter ϵ is evident.

Another physical parameter of the initial stage of stellar evolution that will become accessible to observations in the nearest future is the supernova rate. One of the key projects of the James Webb Space Telescope⁴ is to observe supernovae at high redshifts, $z \sim 10 - 20$. Since at least one supernova may explode in every low-mass halo [36], the number of supernovae at high redshifts should increase if the minimum halo mass is decreased due to the influence of cosmic rays. Figure 5 shows the redshift dependence of the expected specific (per unit mass) supernova rate in the Universe for various values of ϵ , calculated for a standard hierarchical model of galaxy formation within the formalism [35], for the spectrum of perturbations with $n = 1$. The differential mass distribution of the dark halos at a given redshift is

$$\frac{dn}{dM}(M, z) dM = \sqrt{\frac{2}{\pi}} \frac{\delta_c}{D(z) \sigma^2(M)} \frac{d\sigma(M)}{dM} \exp \frac{-\delta_c^2}{2D^2(z) \sigma^2(M)} dM \quad (12)$$

where $D(z)$ is the perturbation growth factor, $\delta_c = 1.69$ is the density parameter, and $\sigma(M)$ is the rms deviation of the perturbations inside mass M . Summing over mass in (12) gives the number of objects per unit comoving volume at redshift z . Estimates of the number of supernovae in a halo are based on currently existing models [37]

$$\gamma(z) = \frac{\nu \Omega_b f_b}{\tau t_{ff}} \simeq 1.2 \times 10^{-7} \Omega_{b,5} f_{b,8} (1+z)_{30}^{3/2} M_6 \text{ yr}^{-1}, \quad (13)$$

where $(1+z)_{30} = (1+z)/30$ and $M_6 = M/10^6 M_\odot$. A Salpeter initial mass function is assumed, which corresponds to one supernova per every $56 M_\odot = \nu^{-1}$, $\Omega_b = 0.05 \Omega_{b,5}$, and $f_b = 0.08 f_{b,8}$ is the fraction of baryons which can cool and form stars [38]. The density of dark matter is $\rho = 200 \rho_c = 200 [1.88 \times 10^{-29} h^2 (1+z)^3]$, and the free-fall time is $t_{ff} = (4\pi G \rho)^{-1/2}$. The efficiency of star formation was normalized to the Galactic value, $\tau^{-1} = 0.6\%$. It is readily seen that at high redshifts, ($z \geq 15$), the number of supernovae grows approximately linearly with ϵ .

4 CONCLUSIONS

We conclude that the increase of the fractional ionization in the post-recombination Universe caused by ultra-high energy cosmic rays, has a stimulating effect on the initial stages of stellar evolution in the Universe: the epoch of the formation of the first stars is shifted to higher redshifts, and the minimum mass for systems in which star formation is possible decreases. This should be manifested in several different observational effects sensitive to the efficiency of UV photon production by the cosmic rays,

¹<http://www.eso.org/projects/alm/>

²<http://www.ir.isas.ac.jp/ASTRO-F>

³<http://safir.jpl.nasa.gov>

⁴<http://www.stsci.edu/jwst/>

ϵ . Considered together, these effects should make it possible to infer the parameters of the UHECR theory or obtain additional constraints for them. These manifestations include emission in rotational lines of H₂ and HD irradiated by contracting protostellar condensations, and the supernova rate and its dependence on redshift. Moreover, enhancement of the initial stage of star formation by cosmic rays can produce additional ionizing photons, which seem currently to be lacking for providing efficient reionization of the Universe.

References

- [1] V.S. Berezinsky, M. Kachelrieß and A. Vilenkin, Phys. Rev. Lett. **79**, 4302 (1997).
- [2] V.A. Kuzmin and V.A. Rubakov, Phys. Atom. Nucl. **61**, 1028 (1998).
- [3] M. Birkel and S. Sarkar, Astropart. Phys. **9**, 298 (1998).
- [4] K. Greisen, Phys. Rev. Lett. **16**, 748 (1966).
- [5] G.T. Zatsepin, V.A. Kuzmin, Pis'ma v JETPh **4**, 114 (1966), [JETP Lett. 4, 78 (1966)].
- [6] A.G. Doroshkevich and P.D. Naselsky, Phys. Rev. D, **12**, 123517 (2002).
- [7] A.G. Doroshkevich, I.P. Naselsky, P.D. Naselsky, I.D. Novikov, Astrophys. J. **586**, 709 (2003).
- [8] W.C. Saslaw, and D. Zipoy, Nature **216**, 967 (1967).
- [9] D. N. Spergel, L. Verde, H.V. Peiris et al., Astophys. J. Suppl. **148**, 175 (2003).
- [10] P.J.E. Peebles, S. Seager, and W. Hu, Astrophys. J. **539**, L1 (2000).
- [11] P. Bhattacharjee, and G. Sigl, Phys. Rept. **327**, 109 (2000).
- [12] M. Tegmark, J. Silk, M.J. Rees, et al., Astophys. J. **474**, 1 (1997).
- [13] J.B. Hutchins, Astrophys. J. **205**, 103 (1976).
- [14] T. Hirasawa, Progr. Theor. Phys. **42**, 523 (1969).
- [15] P.R. Shapiro and H. Kang, Astrophys. J. **318**, 32 (1987).
- [16] Z. Karpas, V. Anicich and W.T. Huntress, J. Chem. Phys. **70**, 2877 (1979).
- [17] D. Galli and F. Palla, Astron. and Astropys. **335**, 403 (1998).
- [18] D. A. Varshalovich and V. K. Khersonskii, Pisma Astron. Zh. 2, 574 (1976) [Sov. Astron. Lett. 2, 227 (1976)].
- [19] Yu. A. Shchekinov, Pisma Astron. Zh. 12, 499 (1986) [Sov. Astron. Lett. 12, 211 (1986)].
- [20] M. Tegmark, J. Silk, A. Evrard, Astrophys. J. **417**, 54 (1993).
- [21] D. Puy and M. Signore, NewA **3**, 247 (1998).
- [22] F. Palla, S.W. Stahler and E.E. Salpeter, Astrophys. J. **271**, 632 (1983).
- [23] S.W. Stahler, F. Palla and E.E. Salpeter, Astrophys. J. **302**, 590 (1986).
- [24] R. Barkana, and A. Loeb, Phys. Rept. **349**, 125 (2001).

- [25] A. Ferrara, *Astrophys. J.* **499**, L17 (1998).
- [26] A. Kogut, D.N. Spergel, C. Barnes, et al., *Astrophys. J. Suppl.* **148**, 161 (2003).
- [27] R. Becker, X. Fan, R.L. White et al., *Astron. J.* **122**, 2850 (2001).
- [28] X. Fan, V.K. Narayanan, M.A. Strauss et al., *Astron. J.* **123**, 1247 (2002).
- [29] R. Cen, *Astrophys. J.* **591**, 12 (2003).
- [30] P. Madau, M.J. Rees, M. Volonteri et al., *Astophys. J.* **604**, 484 (2004)
- [31] R. Cen, *Astrophys. J.* **591**, L5 (2003).
- [32] D.W. Sciama, *Mon. Not. R. Astron. Soc.* **198**, 1 (1982).
- [33] D.W. Sciama, *Phys. Rev. Lett.* **65**, 2839 (1990).
- [34] S.H. Hansen and Z. Haiman, *Astrophys. J.* **600**, 26 (2004).
- [35] W.H. Press and P. Schechter, *Astrophys. J.*, **187**, 425 (1974).
- [36] T. Abel, G.L. Bryan and M. Norman, *Science* **295**, 93 (2002).
- [37] S. Marri, A. Ferrara, L. Pozzetti, *Mon. Not. R. Astron. Soc.* **317**, 265 (2000).
- [38] T. Abel, P. Anninos, Y. Zhang and M.L. Norman, *Astrophys. J.*, **508**, 518 (1998)

Table 1: Chemical-reaction rates.

Reaction	Reaction coefficient k [cm ³ s ⁻¹]	Reference
$H^+ + e^- \rightarrow H + h\nu$	$k_1 \approx 1.88 \times 10^{-10} T^{-0.64}$	[13]
$H + e^- \rightarrow H^- + h\nu$	$k_2 \approx 1.83 \times 10^{-18} T^{0.88}$	[13]
$H^- + H \rightarrow H_2 + e^-$	$k_3 \approx 1.3 \times 10^{-9}$	[14]
$H^+ + H \rightarrow H_2^+ + h\nu$	$k_5 \approx 1.85 \times 10^{-23} T^{1.8}$	[15]
$H_2^+ + H \rightarrow H_2 + H^+$	$k_6 \approx 6.4 \times 10^{-10}$	[16]
$D^+ + H_2 \rightarrow HD + H^+$	$\alpha_1 \approx 2.1 \times 10^{-9}$	[17]
$H^+ + HD \rightarrow H_2 + D^+$	$\alpha_2 \approx \alpha_1 e^{-465 K/T} / 4$	[17]
$H^- + h\nu \rightarrow H + e^-$	$k_4 \approx 0.114 T_\gamma^{2.13} e^{-8650/T_\gamma}$	[17]
$H_2^+ + h\nu \rightarrow H + H^+$	$k_7 \approx 6.365 e^{-71600/T_\gamma}$	[17]

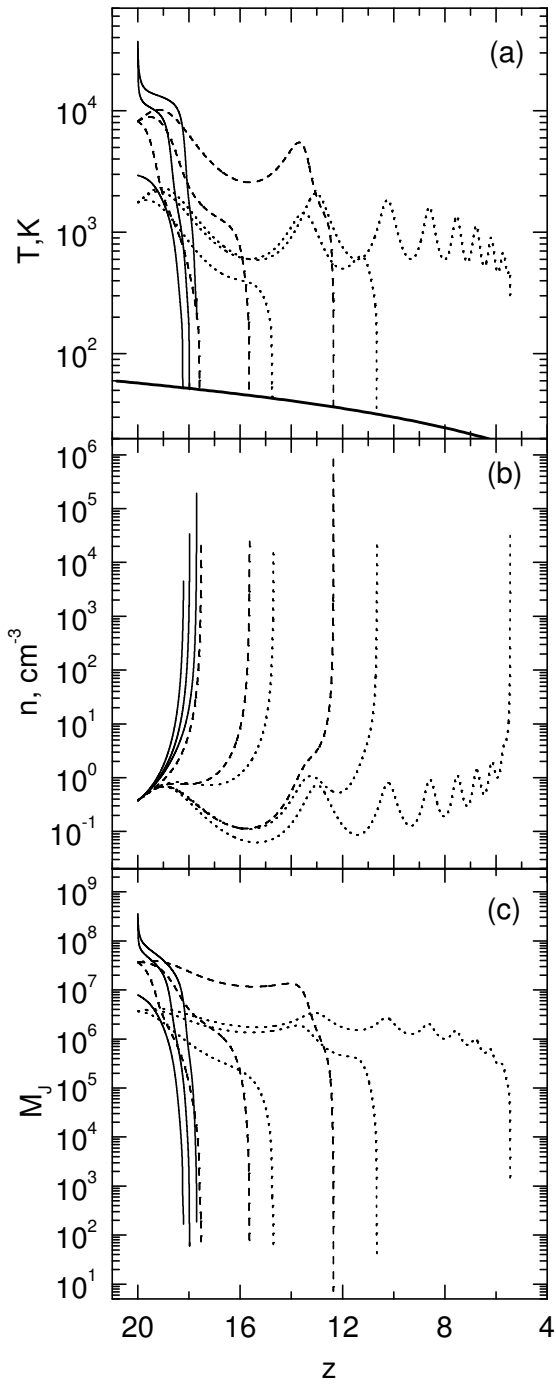


Figure 1: Evolution of the (a) temperature, (b) density, and (c) Jeans mass for three halos with masses of 10^6 (dotted), 10^7 (dashed), and 10^8 (solid) that have reached a virial state at redshift $z = 20$, and for three efficiencies of the production of ionizing photons from cosmic rays, $\epsilon = 0, 0.1, 3$ (from left to right). The solid curve in the upper plot shows the temperature of the CMB.

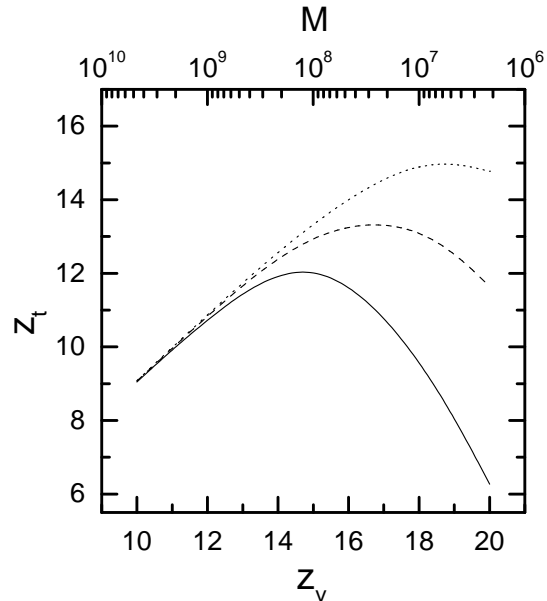


Figure 2: Dependence of the redshift z_t for the transition to a state of isothermal gas contraction on the epoch of halo formation z_v and the efficiency ϵ (the solid, dotted, and dashed curves correspond to $\epsilon = 0, \epsilon = 0.1$, and $\epsilon = 1$, respectively). The plot shows the evolution of a halo with mass $M_{3\sigma}$ corresponding to 3σ perturbation emerged at z_v .

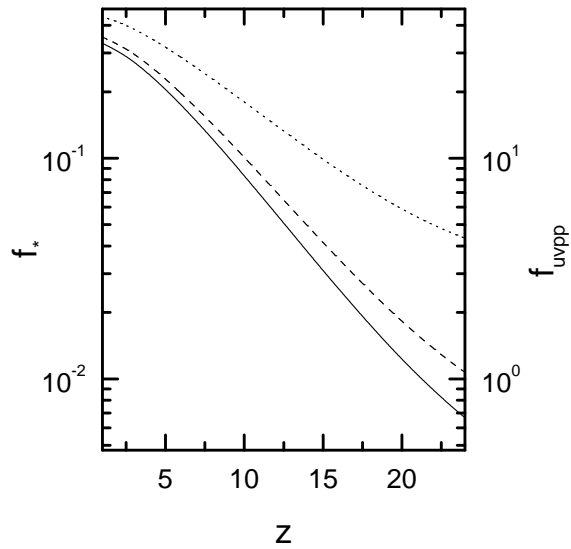


Figure 3: Redshift dependence of the fraction of baryons condensed to a stellar phase in the early star-formation stage in the Universe, f_* , for $\epsilon = 0, 0.1, 1$ (solid, dashed, and dotted, respectively). A standard model for hierarchical clustering is assumed. The scale in the right shows the mean number of ionizing (UV) photons emitted by the stellar population per baryon, f_{uvpp} .

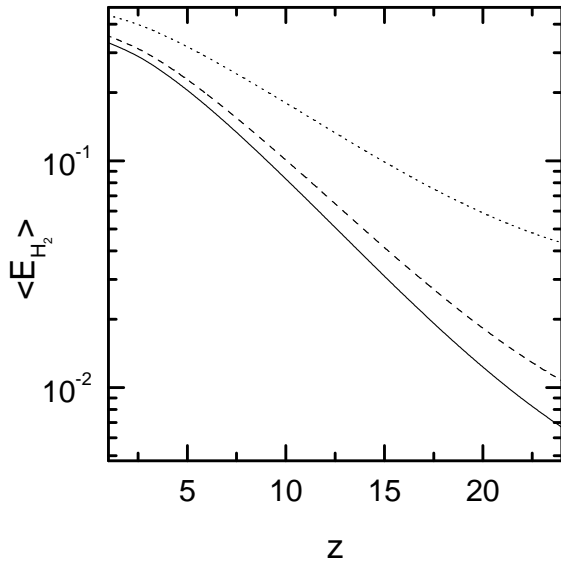


Figure 4: Redshift dependence of the relative specific energy released in H_2 and HD lines for $\epsilon = 0, 0.1, 1$ (solid, dashed, and dotted, respectively). A standard model for hierarchical clustering is assumed.

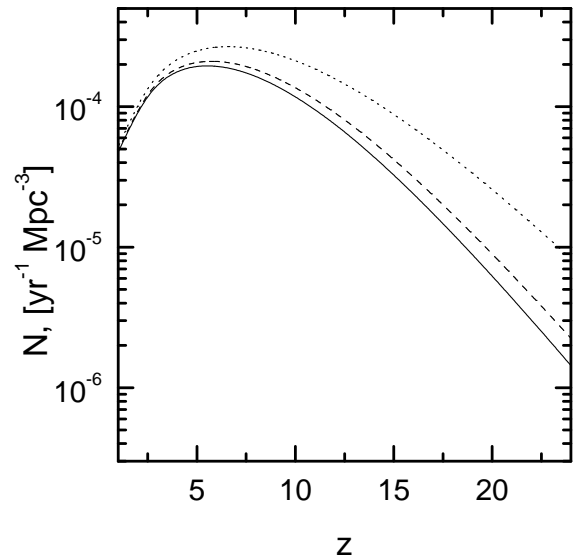


Figure 5: Redshift dependence of the supernova rate for $\epsilon = 0, 0.1, 1$ (solid, dashed, and dotted, respectively). A standard model for hierarchical clustering is assumed.